

# Multiview Self-Representation Learning across Heterogeneous Views

Jie Chen, Member, IEEE, Zhu Wang, Chuanbin Liu, and Xi Peng, Senior Member, IEEE

**Abstract**—Features of the same sample generated by different pretrained models often exhibit inherently distinct feature distributions because of discrepancies in the model pretraining objectives or architectures. Learning invariant representations from large-scale unlabeled visual data with various pretrained models in a fully unsupervised transfer manner remains a significant challenge. In this paper, we propose a multiview self-representation learning (MSRL) method in which invariant representations are learned by exploiting the self-representation property of features across heterogeneous views. The features are derived from large-scale unlabeled visual data through transfer learning with various pretrained models and are referred to as heterogeneous multiview data. An individual linear model is stacked on top of its corresponding frozen pretrained backbone. We introduce an information-passing mechanism that relies on self-representation learning to support feature aggregation over the outputs of the linear model. Moreover, an assignment probability distribution consistency scheme is presented to guide multiview self-representation learning by exploiting complementary information across different views. Consequently, representation invariance across different linear models is enforced through this scheme. In addition, we provide a theoretical analysis of the information-passing mechanism, the assignment probability distribution consistency and the incremental views. Extensive experiments with multiple benchmark visual datasets demonstrate that the proposed MSRL method consistently outperforms several state-of-the-art approaches.

**Index Terms**—Multiview learning, self-representation learning, unsupervised transfer learning, information-passing mechanism.

## I. Introduction

**L**EARNING invariant representations from large-scale visual data with manual annotations often yields human-level performance on downstream tasks such as image recognition [1], object detection [2], and visual tracking [3]. However, obtaining such annotations is extremely expensive and may not be necessary for deep representation learning [4]. Learning invariant representations from large-scale visual data in a fully unsupervised transfer manner presents a significant challenge.

Transfer learning is a fundamental knowledge-transfer technique that in which pretrained deep neural network

J. Chen and X. Peng are with the College of Computer Science, Sichuan University, Chengdu 610065, China. E-mail: chenjie2010@scu.edu.cn; pengx.gm@gmail.com.

C. Liu is with School of Economics and Management, China University of Petroleum (Beijing), Beijing, 100086, China. E-mail: liuchuanbingl@163.com.

Z. Wang is with the Law School, Sichuan University, Chengdu 610065, China. E-mail: wangzhu@scu.edu.cn.

Manuscript received February 5, 2026. This work was supported in part by National Natural Science Foundation of China (NSFC) under Grants 62576231, 62572331 and 72374089, in part by the Natural Science Foundation of Sichuan Province under Grant 2026NSFSC0420, and in part by the Fundamental Research Funds for the Central Universities under Grant 2462025YJRC038.

models are used to improve the performance of the models on target data [5]. Numerous pretrained deep neural network models can provide favorable initialization through transfer learning [6], [7]. The invariant representations learned from large-scale visual data by fine-tuning the entire model can be effectively transferred to various downstream tasks [8], [9]. These methods have shown significant advantages over traditional supervised learning methods. However, substantial performance improvements are observed when the entire vision model is fine-tuned on downstream tasks. In addition, such approaches still require a small number of labeled samples.

Several unsupervised transfer learning methods have been introduced to infer how samples should be labeled in downstream tasks without the need for task-specific representation learning [10], [11]. For example, Alkin et al. [11] introduced a masked image modeling refiner method in which the later blocks of a pretrained model are refined to improve the pretraining objective. Gadetsky et al. [10] proposed an unsupervised transfer learning method to maximize the margins of independent linear classifiers on top of frozen pretrained models. By leveraging foundation vision-language models, these fully unsupervised transfer methods often achieve human-level performance on downstream tasks and outperform fine-tuning-based approaches [12], [13]. However, a significant limitation of these methods lies in the effective capture of complementary information across multiple pretrained models when features are derived from visual data. Complementary information provides additional semantic knowledge preserved across different models. Therefore, learning invariant representations from different pretrained models requires further investigation into how to effectively exploit complementary information across multiple views.

In recent years, contrastive learning has emerged as the dominant paradigm for unsupervised visual representation learning [14], [15], [9]. Contrastive learning aims to learn representations by maximizing a lower bound on the mutual information between the augmented views of visual data, where these augmented views provide complementary information. The objective losses used in contrastive learning techniques, such as InfoNCE [16] and Deep InfoMax [17], explicitly increase the separation between dissimilar pairs of the augmented views while reducing the separation between similar pairs. Many contrastive learning-based methods leverage the generalizability of contrastive learning to obtain compact representations without the need for manually assigned labels [18], [19], [20]. These methods rapidly reduce the performance gap relative to that of supervised learning in large-scale visual data. A pair of augmented views of the same sample is

encoded by the same contrastive learning-based model, resulting in representations that follow a shared underlying distribution [21]. However, features of the same sample generated by different pretrained models may originate from distinct underlying distributions. Therefore, there is an urgent need to learn invariant representations from large-scale unlabeled visual data across heterogeneous views with pretrained models.

In this paper, we propose a multiview self-representation learning (MSRL) method that learns invariant representations from large-scale unlabeled visual data in a fully unsupervised transfer manner. The features are derived from the visual data through transfer learning with different pretrained models. These features are referred to as heterogeneous multiview data. An individual linear model is stacked on top of the corresponding frozen pretrained backbone. We introduce an information-passing mechanism in which self-representation learning is used to aggregate features output by the linear model. Specifically, self-representation learning exploits the self-representation property of features to define a feature aggregation operator that adaptively selects neighborhoods of varying sizes while maintaining the linear weights shared among the features. Each representation corresponding to a feature can be represented by the linear combination of its spatially adjacent neighbors. To learn invariant representations, we present an assignment probability distribution consistency scheme to guide multiview self-representation learning. The assignment probability distributions produced by the linear models contain complementary information across different views, which can provide additional semantic knowledge for clustering assignments. By exploiting complementary information across different views, representation invariance across different views is enforced through the assignment probability distribution consistency scheme. In addition, we provide a theoretical analysis of the information-passing mechanism, the assignment probability distribution consistency and the incremental views. Extensive experiments show that the proposed MSRL method consistently outperforms state-of-the-art approaches across multiple benchmark visual datasets.

The key contributions are summarized as follows.

- An MSRL model is introduced to learn invariant representations from multiple views of large-scale visual data in a fully unsupervised transfer manner.
- An information-passing mechanism is developed to adaptively aggregate feature information. The most linearly related features within the same category are adaptively selected to yield low-dimensional vector representations.
- An assignment probability distribution consistency scheme is introduced for multiview self-representation learning, which exploits additional semantic knowledge to effectively enforce representation invariance across different views.

## II. Related Work

### A. Unsupervised Transfer Learning

In transfer learning, fine-tuning a pretrained model for new downstream tasks has attracted considerable attention because of its demonstrated efficiency and generalizability [7]. However, recent studies have shown that fine-tuning an entire pretrained model on downstream tasks usually leads to faster convergence but results in only marginal improvements over unsupervised transfer learning [10], [9]. Unsupervised transfer learning has become a fundamental paradigm in unsupervised visual representation learning, in which pretrained models are employed to enhance performance on target-specific downstream tasks without the need for labeled samples [11], [12], [13]. Numerous fully unsupervised transfer methods can be divided into two main categories: training a linear classifier on representations generated by frozen pretrained models and parameter-efficient transfer learning techniques that adapt pretrained models to downstream tasks while a limited set of parameters is trained [11], [22]. These methods achieve significant performance improvements by facilitating the adaptation of pre-trained models to downstream tasks.

### B. Multiview Representation Learning

The self-representation property of data samples can be employed to evaluate the membership among data samples if a linear relationship exists among data samples from the same category [23], [24]. Specifically, a sample can be represented as a linear combination of its neighboring samples from the same category. For example, Chen et al. proposed an approximated local linear representation to learn sparse representations on the basis of locality-constrained linear representation learning with probabilistic simplex constraints [25]. Multiview data typically provide both consistent and complementary information across different views of individual data samples. A variety of multiview representation learning methods leverage the self-representation property of data samples to learn a shared representation across multiple views [26], [24]. However, these traditional shallow self-representation models are inadequate for learning discriminative features from large-scale datasets. In contrast, deep self-representation learning models, such as deep autoencoders [27], [28] and graph neural networks [29], [30], [31], exhibit a strong ability to capture intrinsic features within large-scale data. In addition, multiview data generated through data augmentation strategies have been extensively explored in multiview contrastive representation learning approaches [32], [33]. These studies indicate that integrating self-representation learning with deep multiview learning paradigms is crucial for effectively capturing the intrinsic structure of large-scale visual data.

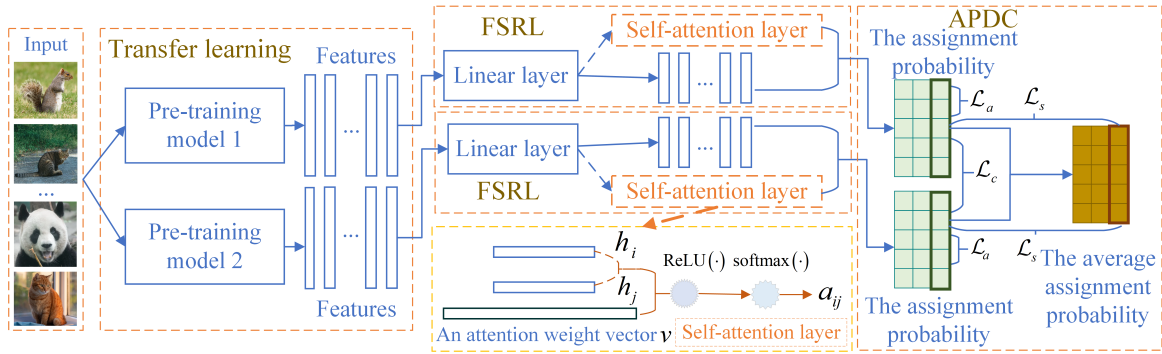


Fig. 1: Framework of the MSRL model with two pretrained models. The framework consists of three main modules: a transfer learning module, a feature self-representation learning (FSRL) module and an assignment probability distribution consistency (APDC) module.

### III. Multiview Self-Representation Learning via Unsupervised Transfer Learning

#### A. Problem Formulation

Given a set of  $M$  pretrained models  $\{\phi_l\}_{l=1}^L$  and an unlabeled dataset  $\mathcal{D} = \{\mathbf{x}_1, \mathbf{x}_2, \dots, \mathbf{x}_n\}$  consisting of  $n$  samples, each pretrained model  $\phi_l(\mathbf{x}_i)$  transforms a raw image  $\mathbf{x}_i$  into a fixed-dimensional vector through transfer learning. For a given pretrained model  $\phi_l$ , a feature self-representation learning (FSRL) model is stacked on top of the fixed-dimensional vectors produced by the frozen pretrained model. Specifically, an FSRL model is denoted as  $\delta^{(l)}(\mathbf{W}_l; \phi_l(\mathbf{x}_i))$ , where  $\mathbf{W}_l$  represents the trainable parameters of the FSRL model. Different pretrained models capture diverse aspects of visual data. Features of the same raw image produced by different pretrained models often exhibit fundamentally distinct feature distributions. The critical challenge lies in learning invariant representations across heterogeneous views from large-scale visual data, while leveraging these pretrained models in a fully unsupervised manner. For simplicity, we consider two pretrained models,  $\phi_i$  and  $\phi_j$ . The parameters  $\mathbf{W}_i$  and  $\mathbf{W}_j$  of the two FSRL models  $\delta^{(i)}(\cdot; \cdot)$  and  $\delta^{(j)}(\cdot; \cdot)$  are jointly learned by the following optimization problem:

$$\min_{\mathbf{W}_i, \mathbf{W}_j} \frac{1}{n} \sum_{r=1}^n \mathcal{L} \left( \delta^{(i)}(\mathbf{W}_i; \phi_i(\mathbf{x}_r)), \delta^{(j)}(\mathbf{W}_j; \phi_j(\mathbf{x}_r)) \right) \quad (1)$$

where  $\mathcal{L}$  represents a general loss function, and the training dataset  $\mathcal{D}_t$  contains  $n$  unlabeled samples, i.e.,  $\mathcal{D}_t = \{\mathbf{x}_1, \mathbf{x}_2, \dots, \mathbf{x}_n\}$ .

#### B. Network Architecture

The network architecture of the MSRL model is illustrated in Fig. 1. It consists of three main modules: a transfer learning module, a feature self-representation learning module and an assignment probability distribution consistency module. The transfer learning module incorporates multiple pretrained models to extract features that capture high-level semantic information from visual data, which results in heterogeneous multiview features.

Given these heterogeneous multiview features, the MSRL framework jointly leverages the self-representation property of these features to learn invariant representations in an unsupervised transfer learning manner.

#### C. Information-Passing Mechanism for Feature Self-Representation Learning

Given a sample  $\mathbf{x} \in \mathbb{R}^m$ , a low-dimensional feature  $\mathbf{h} \in \mathbb{R}^d$  is obtained by applying a linear model  $\sigma(\cdot; \cdot)$  to the output of a pretrained model  $\phi(\mathbf{x})$ , as follows:

$$\mathbf{h} = \sigma(\mathbf{W}^T; \phi(\mathbf{x})) \quad (2)$$

where  $\mathbf{W} \in \mathbb{R}^{d \times C}$  represents the trainable parameters, i.e., the weight matrix of the linear model,  $C$  denotes the number of clusters, and  $\sigma(\cdot; \cdot)$  denotes a linear transformation function. Let  $\mathbf{H} = [\mathbf{h}_1, \mathbf{h}_2, \dots, \mathbf{h}_n] \in \mathbb{R}^{d \times n}$  represent a set of low-dimensional features generated using Eq. (2). The basic assumption on local smoothness is that the features  $\mathbf{H}$  produced by the linear model  $\sigma(\cdot; \cdot)$  can be partitioned into  $C$  clusters by measuring local similarity across each other.

**Assumption III.1 (Local Smoothness).** If two features  $\mathbf{h}_i$  and  $\mathbf{h}_j$  are close to each other, i.e.,  $\mathbf{h}_j \in \mathbb{N}_k(\mathbf{h}_i)$ , in a smooth low-dimensional manifold, their soft cluster assignments are likely to be similar, where  $\mathbb{N}_k(\mathbf{h}_i)$  denotes the set of the  $k$ -nearest neighbors of  $\mathbf{h}_i$ .

The features  $\mathbf{h}_i$  and  $\mathbf{h}_j$  ( $1 \leq i, j \leq n$ ) within the same cluster are linearly dependent. By leveraging the self-representation property of these features, we adopt  $\mathbf{H}$  as the new basis matrix. Thus, each feature  $\mathbf{h}_i$  ( $1 \leq i \leq n$ ) can be represented by the linear combination of  $\mathbf{H}$  as follows:

$$\mathbf{h}_i = \mathbf{H} \mathbf{a}_i + \mathbf{e}_i \quad (3)$$

where  $\mathbf{a}_i \in \mathbb{R}^n$  indicates a coefficient vector of linear combination, and  $\mathbf{e}_i \in \mathbb{R}^d$  is an error term. From the perspective of graph theory, if two features  $\mathbf{h}_i$  and  $\mathbf{h}_j$  are proximate within the intrinsic geometry of the data distribution, their corresponding representations  $\mathbf{a}_i$  and  $\mathbf{a}_j$  are

expected to be similarly proximate under an appropriately defined basis [34]. This relationship indicates that  $\mathbf{a}_i$  and  $\mathbf{a}_j$  are proximate if  $\mathbf{h}_i$  and  $\mathbf{h}_j$  belong to the same cluster.

Each coefficient  $a_{ij}$  in  $\mathbf{a}_i$  is closely associated with the neighbors of the feature  $\mathbf{h}_i$ . To obtain an appropriate coefficient vector  $\mathbf{a}_i$ , we introduce an information-passing mechanism in MSRL. Specifically, information aggregation is performed such that a representation corresponding to each feature is represented by its spatially neighboring features, and their information is leveraged for self-representation. Given a feature  $\mathbf{h}$ , the challenge lies in defining an operator that adaptively selects neighborhoods of varying sizes while maintaining the linear weights shared among the features in  $\mathbf{H}$  within the information-passing mechanism. An attention mechanism is adopted to capture the relationships among the features in  $\mathbf{H}$ , emphasizing the most linearly related features within the same category to produce low-dimensional vector representations [31], [35]. The coefficients  $a_{ij}$  between the features  $\mathbf{h}_i$  and  $\mathbf{h}_j$  computed by the attention mechanism are formulated as follows:

$$a_{ij} = \frac{\exp(\text{ReLU}(\mathbf{v}[\mathbf{h}_i \parallel \mathbf{h}_j]))}{\sum_{r=1}^N \exp(\text{ReLU}(\mathbf{v}[\mathbf{h}_i \parallel \mathbf{h}_r]))} \quad (4)$$

where  $\mathbf{v} \in \mathbb{R}^{2d}$  represents a weight vector learned by a single-layer feed-forward neural network,  $N$  represents the batch size and  $[\cdot \parallel \cdot]$  is the concatenation operation of two features.

The information-passing mechanism allows the representation  $\mathbf{z}_i \in \mathbb{R}^d$ , corresponding to the sample  $\mathbf{x}_i$ , to be formulated as a linear combination of features from the same category, i.e., by aggregating information from spatially proximate neighbors. The aggregation operation of  $\mathbf{h}_i$ , i.e.,  $f(\mathbf{h}_i; \mathbf{a}_i)$ , is defined as follows:

$$\begin{aligned} \mathbf{z}_i &= f(\mathbf{h}_i; \mathbf{a}_i) \\ &= \sum_{j=1}^N a_{ij} \mathbf{h}_j + \mathbf{h}_i. \end{aligned} \quad (5)$$

Through the information-passing mechanism, MSRL aggregates information from neighboring features within the same category to central features, which allows it to effectively capture the geometric structure of these features. Given a pretrained model, the assignment probability distribution of the representation  $\mathbf{z}_i$ , i.e.,  $\mathbf{s}_i \in \Delta^{C-1}$ , corresponding to sample  $\mathbf{x}_i$  ( $1 \leq i \leq n$ ), is calculated as follows:

$$\mathbf{s}_i = \delta(\mathbf{z}_i) \quad (6)$$

where  $\delta(\cdot)$  is a softmax activation function and  $\Delta^{C-1}$  denotes the  $(C-1)$ -dimensional probability simplex, i.e.,

$$\Delta^{C-1} = \left\{ \mathbf{w} \in \mathbb{R}^C : w_i \geq 0, \sum_{i=1}^C w_i = 1 \right\}.$$

#### D. Assignment Probability Distribution Consistency among Multiple Views

Different pretrained models typically yield features with heterogeneous feature distributions for the same sample.

These features are referred to as multiview data. Since they often follow heterogeneous feature distributions, applying contrastive learning directly to them is not suitable for the MSRL model. To overcome this limitation, we present an assignment probability distribution consistency scheme for multiview self-representation learning. The assignment probability distributions produced by the linear models provide additional semantic knowledge for cluster assignments. In particular, these assignment probability distributions contain complementary information across different views.

The linear models corresponding to the pretrained models are expected to yield the same cluster assignment. Given  $L$  pretrained models, a latent semantic assignment probability distribution for a sample  $\mathbf{x}_i$  across the linear models is calculated as follows:

$$\rho_\theta(\mathbf{x}_i) = \frac{1}{L} \sum_{l=1}^L \mathbf{s}_i^{(l)} \quad (7)$$

where  $\mathbf{s}_i^{(l)} = \delta_l(f_l(\sigma_l((\mathbf{W}_k)^T; \phi_l(\mathbf{x}_i)); \mathbf{a}_i^{(l)}))$ . The cluster assignment of sample  $\mathbf{x}_i$  can be predicted by

$$y_i = \arg \max_j [\rho_\theta(\mathbf{x}_i)]_j, \quad j \in [1, 2, \dots, C] \quad (8)$$

where  $[\rho_\theta(\mathbf{x}_i)]_j$  represents the assignment probability distribution of a sample  $\mathbf{x}_i$  to the  $j$ th cluster. The cluster assignment provides specific semantic knowledge for generating pseudolabel. Under the guidance of these assignments, the semantic pseudolabel loss for unlabeled samples is formulated as follows:

$$\mathcal{L}_s = \frac{1}{B} \sum_{i=1}^B \frac{1}{L} \sum_{l=1}^L \mathcal{H}(y_i, \mathbf{s}_i^{(l)}) \quad (9)$$

where  $\mathcal{H}(\cdot, \cdot)$  is the cross-entropy loss, i.e.,  $\mathcal{H}(y_i, \mathbf{s}_i^{(l)}) = -\log \mathbf{s}_{i,y_i}^{(l)}$ , and  $B$  denotes the batch size of the unlabeled samples. The assignment probability distributions produced by all linear models  $\{\mathbf{s}_i^{(l)}\}_{l=1}^L$  for sample  $\mathbf{x}_i$  are directed toward the same probability direction, which indicates that these assignment probability distributions are jointly attracted toward the consensus  $\rho_\theta(\mathbf{x}_i)$ . Therefore, the consensus distribution is a stable attractor for all linear models.

To avoid all samples being assigned to a single cluster, we introduce the following regularization term:

$$\mathcal{L}_a = \sum_{l=1}^L \sum_{j=1}^C q_j^{(l)} \log q_j^{(l)} \quad (10)$$

where  $q_j^{(l)}$  is defined as follows:

$$q_j^{(l)} = \frac{1}{B} \sum_{i=1}^B s_{ij}^{(l)}. \quad (11)$$

This term is considered a cluster diversity loss in the MSRL model [36], which promotes balanced cluster assignments by maximizing the cross-entropy loss of the probability assignment for each FSRL component.

**Algorithm 1 Optimization Procedure for MSRL**

Input: An unlabeled dataset  $\mathcal{D} = \{\mathbf{x}_1, \mathbf{x}_2, \dots, \mathbf{x}_n\}$  with  $C$  categories.  
 Parameter: The number of iterations  $epochs$ , parameters  $\alpha > 0$  and  $\beta > 0$ .  
 Output: The predicted labels of the unlabeled dataset  $\mathcal{D}$   
 $\mathbf{Y} = [y_1, y_2, \dots, y_n]$ .

---

- 1: for  $t = 1$  to  $epochs$  do
- 2:   Obtaining a set of features  $\mathbf{H}$  via Eq. (2);
- 3:   Obtaining the representations of the features  $\mathbf{Z}$  via Eq. (5) using the information-passing mechanism;
- 4:   Determining the assignment probability distribution of each unlabeled sample  $s_i$  produced by the  $k$ th component of the MSRL model via Eq. (6);
- 5:   Determining the cluster assignment of each unlabeled sample  $y_i$  via Eq. (8);
- 6:   Updating the whole network by minimizing  $\mathcal{L}$  in Eq. (14);
- 7: end for
- 8: Determining  $y_i$  via Eq. (8) for each unlabeled sample in  $\mathcal{D}$ .

---

The consistency loss is an important component widely used in various self-supervised learning algorithms. The features from different views tend to share consistent assignment probability distributions. By minimizing the discrepancy among the assignment probability distributions produced by multiple linear models, the generalizability of the linear models is enhanced. The cross-view consistency loss over assignment probability distributions is defined as follows:

$$\mathcal{L}_c = \frac{1}{B} \sum_{i=1}^B \sum_{p=1}^L \sum_{q=1, p \neq q}^L \mathcal{H} \left( \mathbf{s}_i^{(p)}, \mathbf{s}_i^{(q)} \right) \quad (12)$$

where  $\mathbf{s}_i^{(p)}$  and  $\mathbf{s}_i^{(q)}$  are the assignment probability distributions produced by the  $p$ th and  $q$ th linear models, respectively. The cross-entropy between  $\mathbf{s}_i^{(p)}$  and  $\mathbf{s}_i^{(q)}$  is given by

$$\mathcal{H} \left( \mathbf{s}_i^{(p)}, \mathbf{s}_i^{(q)} \right) = - \sum_{j=1}^C s_{ij}^{(p)} \log s_{ij}^{(q)}. \quad (13)$$

Eq. (13) drives the assignments of different views for each sample to converge in the probability simplex, which leads to refined alignment across multiple views.

The MSRL model employs three complementary loss components, i.e., the semantic pseudolabel loss, the cluster diversity loss and the cross-view consistency loss, that jointly enforce assignment probability distribution consistency among the linear models. The overall loss objective of the MSRL model is given as follows:

$$\mathcal{L} = \mathcal{L}_s + \alpha \mathcal{L}_a + \beta \mathcal{L}_c \quad (14)$$

where  $\alpha$  and  $\beta$  are tradeoff hyperparameters. The assignment probability distributions produced by different linear models associated with heterogeneous pretrained

backbones converge to a unified distribution. An adaptive momentum-based mini-batch gradient descent method [37] is used to optimize the entire network while keeping the pretrained models frozen. The entire optimization procedure of the proposed MSRL method is provided in Algorithm 1.

**E. Theoretical Justification**

In this section, we provide theoretical discussions to clarify multiview self-representation learning and its connections with the information-passing mechanism, assignment probability distribution consistency and incremental views.

**1) Information-Passing Mechanism:**

**Definition III.2 (Weak Neighborhood Alignment).** The encoder  $f$  is weakly neighborhood-aligned if for any neighboring representation pair  $\mathbf{z}_i$  and  $\mathbf{z}_j$ , the following condition is satisfied, i.e.,

$$\mathbb{E}_{j \in \mathbb{N}_k(i)} \|\mathbf{z}_i - \mathbf{z}_j\|_2 \leq \varepsilon$$

where  $\mathbf{x}_j \in \mathbb{N}_k(\mathbf{x}_i)$  and  $\varepsilon > 0$  is a small constant.

According to Definition III.2, the difference between the representations corresponding to neighboring features approximately lies in the null space of the weight matrix  $\mathbf{W}$  of the shared linear layer. If row normalization is applied to  $\mathbf{W}$ , the following inequality holds:

$$\begin{aligned} & \|\mathbf{W}(\phi(\mathbf{x}_i) - \phi(\mathbf{x}_j))\|_2 \\ & \leq \sqrt{C} \|\phi(\mathbf{x}_i) - \phi(\mathbf{x}_j)\|_2. \end{aligned} \quad (15)$$

Row normalization mitigates undesired amplification along specific directions, making attention computation more stable. Consequently, the weak neighborhood alignment condition is more reliably satisfied in self-representation learning.

**Theorem III.3 (Local Neighborhood Alignment).** Let  $\mathbf{h}_i$  and  $\mathbf{h}_j$  be a neighboring feature pair, and let  $s_i = \delta(f(\mathbf{h}_i; \mathbf{a}_i))$  and  $s_j = \delta(f(\mathbf{h}_j; \mathbf{a}_j))$  be their corresponding assignment probability distributions, where  $\delta(\cdot)$  is the softmax activation function and  $f(\cdot; \cdot)$  represents an aggregation operation. The following equality holds:

$$\mathbf{s}_i = \mathbf{s}_j$$

if the following condition is satisfied:

$$f(\mathbf{h}_i; \mathbf{a}_i) - f(\mathbf{h}_j; \mathbf{a}_j) = c\mathbf{1}$$

where  $c \in \mathbb{R}$  is a constant.

**Proof.** The softmax function is translation invariant, i.e., for any scalar  $\mu \in \mathbb{R}$ ,

$$\text{softmax}(\mu + c\mathbf{1}) = \text{softmax}(\mu).$$

Thus, it follows that

$$\begin{aligned} \mathbf{s}_i &= \delta(f(\mathbf{h}_i; \mathbf{a}_i)) \\ &= \delta(f(\mathbf{h}_j; \mathbf{a}_j) + c\mathbf{1}) \\ &= \delta(f(\mathbf{h}_j; \mathbf{a}_j)) \\ &= \mathbf{s}_j. \end{aligned}$$

□ By taking expectations with respect to  $\mathbf{s}_i^{(l)}$ , we get

$$\begin{aligned}\mathbb{E} \left[ \mathcal{H} \left( \mathbf{p}_i^{(L)} \right) \right] &\leq \mathbb{E} \left[ \frac{1}{L} \sum_{l=1}^L \mathcal{H} \left( \mathbf{s}_i^{(l)} \right) \right] \\ &= \frac{1}{L} \sum_{l=1}^L \mathbb{E} \left[ \mathcal{H} \left( \mathbf{s}_i^{(l)} \right) \right].\end{aligned}$$

According to the assumption, we obtain

$$\begin{aligned}\mathbb{E} \left[ \left\| \mathbf{s}_i^{(l)} - \mathbf{p}_i^{(L)} \right\|_1 \right] &= \mathbb{E} \left[ \left\| \mathbf{s}_i^{(l)} - \frac{1}{L} \sum_{r=1}^L \mathbf{s}_i^{(r)} \right\|_1 \right] \\ &\leq \frac{1}{L} \sum_{r=1}^L \mathbb{E} \left[ \left\| \mathbf{s}_i^{(l)} - \mathbf{s}_i^{(r)} \right\|_1 \right] \\ &\leq \varepsilon.\end{aligned}$$

As  $\mathcal{H}(\cdot)$  is Lipschitz-continuous on the probability simplex  $\Delta_{\delta}^{C-1}$ , there exists a constant  $Q_{\delta} > 0$  for any two variables  $\mathbf{u} \in \Delta_{\delta}^{C-1}$  and  $\mathbf{v} \in \Delta_{\delta}^{C-1}$  such that

$$|\mathcal{H}(\mathbf{u}) - \mathcal{H}(\mathbf{v})| \leq Q_{\delta} (\|\mathbf{u} - \mathbf{v}\|_1).$$

Thus,

$$\left| \mathbb{E} \left[ \mathcal{H} \left( \mathbf{p}_i^{(L)} \right) \right] - \mathbb{E} \left[ \mathcal{H} \left( \mathbf{s}_i^{(l)} \right) \right] \right| \leq Q_{\delta} \varepsilon.$$

Finally,

$$\mathbb{E} \left[ \mathcal{H} \left( \mathbf{p}_i^{(L)} \right) \right] - \frac{1}{L} \sum_{l=1}^L \mathbb{E} \left[ \mathcal{H} \left( \mathbf{s}_i^{(l)} \right) \right] \leq Q_{\delta} \varepsilon.$$

□

The semantic pseudolabel loss in Eq. (9) is minimized when the assignment probability distribution is concentrated on the same category  $y_i$  for all pretrained models, where  $y_i$  is computed from  $\rho_{\theta}(\mathbf{x}_i)$ . Theorem III.4 establishes two fundamental properties of assignment probability distribution consistency. Specifically, information fusion of assignment probability distributions across multiple views is effectively achieved in the probability simplex by averaging assignment probability distributions. Moreover, under the assumption that the disagreement among view-specific assignment probability distributions is bounded, the entropy of the fused assignment probability distribution is strictly reduced, providing a theoretical guarantee of the fused assignment probability distribution. Therefore, the assignment probability distributions  $\mathbf{s}_i^{(l)}$  of all linear models converge to the latent semantic assignment distribution  $\mathbf{p}_i^{(L)}$  for sample  $\mathbf{x}_i$ .

3) Incremental View Analysis: We present a view-incremental theoretical analysis to characterize how clustering quality evolves as heterogeneous views corresponding to different pretrained models are progressively introduced into MSRL. Specifically, when a new pretrained model is incorporated into an existing collection of  $L$  pretrained models, the latent semantic assignment probability distribution  $\mathbf{p}_i^{(L+1)}$  for a sample  $\mathbf{x}_i$  over the  $(L+1)$  linear models is updated in an incremental manner. Such incrementally incorporated heterogeneous views define

Theorem III.3 indicates that when the encoder  $f$  is weakly neighborhood-aligned, neighboring features can share an identical assignment probability distribution. This result follows directly from the translation invariance of the softmax function. Furthermore, let  $\mathbf{z}_i = f(\sigma(\mathbf{W}^T; \phi(\mathbf{x}_i)); \mathbf{a}_i)$  and  $\mathbf{z}_j = f(\sigma(\mathbf{W}^T; \phi(\mathbf{x}_j)); \mathbf{a}_j)$  be two representations corresponding to a pair of neighboring samples  $\mathbf{x}_i$  and  $\mathbf{x}_j$ , respectively. Here  $\mathbf{z}_i$  and  $\mathbf{z}_j$  are considered invariant representations for  $\mathbf{x}_i$  and  $\mathbf{x}_j$ , respectively. These representations become strictly neighborhood-aligned, i.e.,  $\mathbf{z}_i = \mathbf{z}_j$  when the linear model satisfies  $\text{rank}(\mathbf{W}) = d$  and  $d \leq C$ . However, the opposite condition, i.e.,  $d > C$ , often holds in high-dimensional data. This finding indicates that  $\mathbf{W}$  cannot enforce strict neighborhood alignment. In contrast, weak neighborhood alignment provides more realistic and appropriate conditions for the information-passing mechanism.

## 2) Assignment Probability Distribution Consistency:

Let  $\left\{ \mathbf{s}_i^{(l)} \right\}_{l=1}^L \in \Delta_{\delta}^{C-1}$  denote the assignment probability distributions produced by the  $L$  linear models for sample  $\mathbf{x}_i$ , where  $\Delta_{\delta}^{C-1}$  is the probability simplex, i.e.,  $\Delta_{\delta}^{C-1} = \{ \mathbf{w} \in \Delta^{C-1} : w_i \geq \delta > 0 \}$ . As  $\mathbf{s}_i^{(l)}$  is generated by a softmax operator in Eq. (6), it lies in the interior of the probability simplex. In particular, the entropy function  $\mathcal{H}(\cdot)$  is Lipschitz-continuous in this domain. For fixed  $\mathbf{s}_i^{(p)}$ , the cross-entropy  $\mathcal{H}(\mathbf{s}_i^{(p)}, \mathbf{s}_i^{(q)})$  in Eq. (12) is strictly convex in  $\mathbf{s}_i^{(q)}$  and uniquely minimized when  $\mathbf{s}_i^{(p)} = \mathbf{s}_i^{(q)}$ .

Theorem III.4 (Bounded Multiview Consistency). Considering the sample  $\mathbf{x}_i$ , assume that there exists a sufficiently small constant  $\varepsilon > 0$  such that

$$\mathbb{E} \left[ \left\| \mathbf{s}_i^{(p)} - \mathbf{s}_i^{(q)} \right\|_1 \right] \leq \varepsilon, \quad \forall p \neq q$$

where  $\mathbf{s}_i^{(p)} \in \Delta_{\delta}^{C-1}$  and  $\mathbf{s}_i^{(q)} \in \Delta_{\delta}^{C-1}$  denote the assignment probability distributions produced by the  $p$ th and  $q$ th linear models, respectively. Then, there exists a latent semantic assignment probability distribution  $\mathbf{p}_i^{(L)} \in \Delta_{\delta}^{C-1}$  for sample  $\mathbf{x}_i$  over  $L$  linear models, defined as  $\mathbf{p}_i^{(L)} = \rho_{\theta}(\mathbf{x}_i)$ , which satisfies the following properties:

$$\begin{aligned}(1) \quad \mathbb{E} \left[ \mathcal{H} \left( \mathbf{p}_i^{(L)} \right) \right] &\leq \frac{1}{L} \sum_{l=1}^L \mathbb{E} \left[ \mathcal{H} \left( \mathbf{s}_i^{(l)} \right) \right] + Q_{\delta} \varepsilon; \\ (2) \quad \mathbb{E} \left[ \left\| \mathbf{s}_i^{(l)} - \mathbf{p}_i^{(L)} \right\|_1 \right] &\leq \varepsilon, \quad \forall l = 1, \dots, L\end{aligned}$$

where  $L$  denote the number of pretrained models, and  $Q_{\delta} > 0$  is the Lipschitz constant of the entropy function on the probability simplex  $\Delta_{\delta}^{C-1}$ .

Proof. For any deterministic distributions  $\left\{ \mathbf{s}_i^{(l)} \right\}_{l=1}^L$ , we have

$$\mathcal{H} \left( \frac{1}{L} \sum_{l=1}^L \mathbf{s}_i^{(l)} \right) \leq \frac{1}{L} \sum_{l=1}^L \mathcal{H} \left( \mathbf{s}_i^{(l)} \right).$$

an incremental consensus dynamical system. According to Eq. (7), the latent semantic assignment distribution  $\mathbf{p}_i^{(L+1)}$  for sample  $\mathbf{x}_i$  is updated incrementally as follows:

$$\mathbf{p}_i^{(L+1)} = \frac{L}{L+1} \mathbf{p}_i^{(L)} + \frac{1}{L+1} \mathbf{s}_i^{(L+1)} \quad (16)$$

where  $\mathbf{p}_i^{(L)}$  is defined as  $\mathbf{p}_i^{(L)} = \rho_\theta(\mathbf{x}_i)$  with  $L$  pretrained models and  $\mathbf{s}_i^{(L+1)}$  denotes the assignment probability distribution produced by the  $(L+1)$ th linear model. This defines an incremental updating rule for the latent semantic assignment probability distribution.

**Assumption III.5 (Bounded Multiview Discrepancy).** Given a sample  $\mathbf{x}_i$ , assume that there exists a sufficiently small constant  $\varepsilon > 0$  such that, for each view  $l$ ,

$$\mathbb{E} [\|\mathbf{s}_i^{(l)} - \mathbf{p}_i\|_1] \leq \varepsilon, \quad \forall l = 1, \dots, L$$

where  $\mathbf{p}_i \in \Delta_\delta^{C-1}$  denotes a consensus assignment probability distribution,  $\mathbf{s}_i^{(l)} \in \Delta_\delta^{C-1}$  represents the assignment probability distribution produced by the  $l$ th linear model, and  $L$  denote the number of pretrained models.

**Theorem III.6 (Robbins-Monro Stochastic Approximation [38]).** Let  $\{u_t\}_{t \geq 1}$  be a sequence of nonnegative random variables satisfying the recursive inequality

$$\mathbb{E}[u_{t+1}] \leq (1 - \alpha_t) \mathbb{E}[u_t] + \alpha_t \varepsilon$$

where  $\varepsilon \geq 0$  is a constant and  $\{\alpha_t\}_{t \geq 1}$  is a deterministic step-size sequence satisfying

$$\alpha_t > 0, \quad \sum_{t=1}^{\infty} \alpha_t = \infty \quad \text{and} \quad \sum_{t=1}^{\infty} \alpha_t^2 < \infty.$$

Then, the sequence  $\{\mathbb{E}[u_t]\}$  is uniformly bounded and converges to a neighborhood of size  $\varepsilon$ . More precisely, there exists a constant  $w > 0$ , depending only on the initial value  $u_1$ , such that

$$\mathbb{E}[u_t] \leq w \prod_{k=1}^{t-1} (1 - \alpha_k) + \varepsilon \sum_{k=1}^{t-1} \alpha_k \prod_{j=k+1}^{t-1} (1 - \alpha_j).$$

In particular, when  $\alpha_t = 1/t$ , it holds that

$$\mathbb{E}[u_t] \leq \mathcal{O}\left(\frac{1}{t}\right) + \varepsilon.$$

**Theorem III.7 (Attractivity of Consensus Distribution).** Under Assumption (III.5), there exists a constant  $w > 0$  such that

$$\mathbb{E} [\|\mathbf{p}_i^{(L)} - \mathbf{p}_i\|_1] \leq w \left( \frac{1}{L} + \varepsilon \right)$$

where  $\mathbf{p}_i^{(L)}$  is a latent semantic assignment probability distribution for the sample  $\mathbf{x}_i$  over  $L$  linear models.

**Proof.** A residual term is defined as

$$\mathbf{e}_i^{(L)} = \mathbf{p}_i^{(L)} - \mathbf{p}_i.$$

By the incremental updating rule in Eq. (16), we obtain

$$\mathbf{e}_i^{(L+1)} = \frac{L}{L+1} \mathbf{e}_i^{(L)} + \frac{1}{L+1} (\mathbf{s}_i^{(L+1)} - \mathbf{p}_i)$$

Taking the  $l_1$ -norm and expectation on both sides, and applying the triangle inequality, we have

$$\begin{aligned} \mathbb{E} [\|\mathbf{e}_i^{(L+1)}\|_1] &\leq \frac{L}{L+1} \mathbb{E} [\|\mathbf{e}_i^{(L)}\|_1] \\ &\quad + \frac{1}{L+1} \mathbb{E} [\|\mathbf{s}_i^{(L+1)} - \mathbf{p}_i\|_1]. \end{aligned}$$

By Assumption (III.5), we further have

$$\begin{aligned} \mathbb{E} [\|\mathbf{e}_i^{(L+1)}\|_1] &\leq \frac{L}{L+1} \mathbb{E} [\|\mathbf{e}_i^{(L)}\|_1] + \frac{\varepsilon}{L+1} \\ &= \mathbb{E} [\|\mathbf{e}_i^{(L)}\|_1] - \frac{1}{L+1} (\mathbb{E} [\|\mathbf{e}_i^{(L)}\|_1] - \varepsilon) \end{aligned}$$

This recursive inequality corresponds to a Robbins-Monro stochastic approximation, and we get

$$\mathbb{E} [\|\mathbf{e}_i^{(L)}\|_1] \leq w \left( \frac{1}{L} + \varepsilon \right)$$

for some constant  $w > 0$ , which is independent of  $L$ .  $\square$

**Theorem III.7** indicates that the latent semantic assignment probability distribution  $\mathbf{p}_i^{(L)}$  is attracted to the consensus assignment probability distribution  $\mathbf{p}_i$  as  $L$  increases. In particular, the effect of stochastic perturbations remains bounded by  $\mathcal{O}(\varepsilon)$ . Consequently,  $\mathbf{p}_i$  is regarded as a stable attractor in expectation for an incremental consensus dynamic system. This attractor property explains why the latent semantic assignment probability distribution  $\mathbf{p}_i^{(L)}$  stabilizes as  $L$  increases under Assumption (III.5). In addition, Theorem III.7 characterizes how uncertainty evolves along the attracting trajectory.

**Theorem III.8 (Monotonic Entropy Reduction).** Under Assumption (III.5), the expected entropy of  $\mathbf{p}_i^{(L+1)}$  for the sample  $\mathbf{x}_i$  satisfies

$$\mathbb{E} [\mathcal{H}(\mathbf{p}_i^{(L+1)})] - \mathbb{E} [\mathcal{H}(\mathbf{p}_i^{(L)})] \leq \frac{2Q_\delta \varepsilon}{L+1},$$

where  $\mathbf{p}_i^{(L)}$  is a consensus assignment probability distribution for the sample  $\mathbf{x}_i$  over the  $L$  linear models, and  $Q_\delta > 0$  is the Lipschitz constant of the entropy function on the probability simplex  $\Delta_\delta^{C-1}$ .

**Proof.** By applying the incremental updating rule in Eq. (16) and leveraging the concavity of entropy on the probability simplex, we obtain

$$\mathcal{H}(\mathbf{p}_i^{(L+1)}) \leq \frac{L}{L+1} \mathcal{H}(\mathbf{p}_i^{(L)}) + \frac{1}{L+1} \mathcal{H}(\mathbf{s}_i^{(L+1)}).$$

Furthermore, we get

$$\begin{aligned} \mathcal{H}(\mathbf{p}_i^{(L+1)}) - \mathcal{H}(\mathbf{p}_i^{(L)}) &\leq \frac{1}{L+1} (\mathcal{H}(\mathbf{s}_i^{(L+1)}) - \mathcal{H}(\mathbf{p}_i^{(L)})). \end{aligned}$$

By the triangle inequality and the assumption, we get

$$\begin{aligned} \mathbb{E} [\|\mathbf{s}_i^{(L+1)} - \mathbf{p}_i^{(L)}\|_1] &\leq \mathbb{E} [\|\mathbf{s}_i^{(L+1)} - \mathbf{p}_i\|_1] + \mathbb{E} [\|\mathbf{p}_i^{(L)} - \mathbf{p}_i\|_1] \\ &\leq \mathbb{E} [\|\mathbf{s}_i^{(L+1)} - \mathbf{p}_i\|_1] + \mathbb{E} \left[ \left\| \frac{1}{L} \sum_{l=1}^L (\mathbf{s}_i^{(l)} - \mathbf{p}_i) \right\|_1 \right] \\ &\leq 2\varepsilon. \end{aligned}$$

TABLE I: Statistics of the graph datasets.

Name	Train	Test	Classes
Pets	3,680	3,669	37
GTSRB	26,640	12,630	43
DTD	3,760	1,880	47
Aircraft	6,667	3,333	100
Flowers	2,040	6,149	102
CIFAR-10	50,000	10,000	10
CIFAR-100	50,000	10,000	100
ImageNet-100	1,281,167	50,000	1,000

As  $\mathcal{H}(\cdot)$  is Lipschitz-continuous on the probability simplex  $\Delta_{\delta}^{C-1}$ , there exists a constant  $Q_{\delta} > 0$  for any two variables  $\mathbf{u} \in \Delta_{\delta}^{C-1}$  and  $\mathbf{v} \in \Delta_{\delta}^{C-1}$  such that

$$|\mathcal{H}(\mathbf{u}) - \mathcal{H}(\mathbf{v})| \leq Q_{\delta} (\|\mathbf{u} - \mathbf{v}\|_1).$$

Thus,

$$\begin{aligned} & \mathbb{E} \left[ \mathcal{H} \left( \mathbf{p}_i^{(L+1)} \right) \right] - \mathbb{E} \left[ \mathcal{H} \left( \mathbf{p}_i^{(L)} \right) \right] \\ & \leq \frac{1}{L+1} \left( \mathbb{E} \left[ \mathcal{H} \left( \mathbf{s}_i^{(L+1)} \right) \right] - \mathbb{E} \left[ \mathcal{H} \left( \mathbf{p}_i^{(L)} \right) \right] \right) \\ & \leq \frac{Q_{\delta}}{L+1} \mathbb{E} \left[ \|\mathbf{s}_i^{(L+1)} - \mathbf{p}_i^{(L)}\|_1 \right] \\ & \leq \frac{2Q_{\delta}\varepsilon}{L+1}. \end{aligned}$$

□

Theorem III.8 characterizes the entropy evolution of the consensus assignment probability distribution under incremental heterogeneous views. Specifically, when the assignment probability distributions produced by individual linear models are mutually consistent up to a bounded deviation, the change in entropy induced by incorporating an additional view is tightly controlled. This result also indicates that not every additional view is guaranteed to be beneficial. In addition, Theorem III.8 establishes that the expected entropy variation decays at a rate of  $\mathcal{O}(\varepsilon/(L+1))$ . This implies that as more heterogeneous views are aggregated, the consensus assignment probability distribution becomes increasingly stable in terms of uncertainty, and any potential increase in entropy vanishes asymptotically. From the perspective of the incremental consensus dynamical system, this result indicates that the incremental update on the consensus assignment probability distribution forms a stabilizing process in the probability simplex, which prevents entropy inflation caused by heterogeneous views.

#### IV. Experiments

In this section, we conduct extensive experiments to evaluate the performance of the proposed MSRL method. All the experiments are conducted on a Linux workstation equipped with a GeForce RTX 4090 GPU (24 GB caches), an Intel(R) Xeon(R) Platinum 8336C CPU, and 128.0 GB of RAM.

#### A. Experimental Settings

Following the experimental settings in the previous work [10], two representative pretrained models, i.e., DINOv2 [39] and CLIP ViT-L/14 [40], are employed as backbones to derive two corresponding augmented feature views. We evaluate the clustering performance of MSRL on eight publicly available vision datasets, namely, the Pets, GTSRB, DTD, Aircraft, Flowers, CIFAR-10, CIFAR-100 and ImageNet-100 datasets [41]. The statistics of the datasets are presented in Table I. Each dataset is divided into two subsets: the training set and the test set. Two types of unsupervised transfer learning tasks, namely, self-supervised learning and zero-shot transfer learning, are employed for performance evaluation. To evaluate the effectiveness of the proposed MSRL method on self-supervised learning, we compare the proposed MSRL method against state-of-the-art approaches, namely, simple contrastive multiview clustering (SCMVC) [33], contrastive multiview clustering (CMVC) [42], sparse multiview clustering (SparseMVC) [43], hierarchical semantic alignment and cooperative completion (HSACC) [44], multilevel contrastive multiview clustering [45] and TURTLE [10]. In addition, CLIP zero-shot transfer [10] and LaFTer [13] are included as baselines for comparison in the zero-shot transfer learning task. The source code for MSRL is implemented using the PyTorch framework [41]. The source code <sup>1</sup> for MSRL is publicly available online. The source code for all the comparison algorithms is provided by their respective authors. Four standard metrics are employed to evaluate the clustering performance of all the competing methods, i.e., the clustering accuracy (ACC), normalized mutual information (NMI) and adjusted rand index (ARI). For these metrics, a higher value indicates better clustering performance.

The learning rate for the proposed MSRL model was empirically set to  $5e^{-4}$  for the GTSRB, DTD and CIFAR-100 datasets, and to  $1e^{-3}$  for the remaining datasets. The batch size of each dataset was chosen from the range of  $\{10,000, 5,000, 1,000, 500, 100\}$  during training and testing, depending on the number of samples in the dataset. The dropout rate was set to 0.1. The overall loss of the proposed MSRL model in Eq. (14) involves two hyperparameters,  $\alpha$  and  $\beta$ . The hyperparameter  $\alpha$  was selected from  $\{1.0, 5.0, 10.0\}$  via a linear search strategy, while  $\beta$  was fixed at 1.0. To ensure a fair comparison, we report the best performance of all the competing methods after hyperparameter tuning.

#### B. Performance Evaluation

In this section, we conduct an experimental evaluation on two types of unsupervised transfer learning tasks, namely, self-supervised learning and zero-shot transfer learning. These tasks are employed to evaluate the generalizability of the proposed MSRL model under different levels of unsupervised transfer learning.

<sup>1</sup><https://github.com/chenjie20/MSRL>

TABLE II: Clustering performance of the different methods on eight vision datasets.

Methods	Pets			GTSRB			DTD			Aircraft			Flowers			CIFAR-10			CIFAR-100			ImageNet		
	ACC	NMI	ARI	ACC	NMI	ARI	ACC	NMI	ARI	ACC	NMI	ARI	ACC	NMI	ARI	ACC	NMI	ARI	ACC	NMI	ARI	ACC	NMI	ARI
SCMVC	84.04	90.24	79.47	21.57	34.09	11.94	55.59	62.66	38.89	16.77	44.69	14.19	97.17	99.17	98.02	80.31	75.42	64.75	75.96	81.52	62.59	-	-	-
CMVC	90.30	92.29	84.20	31.12	57.45	25.17	54.36	66.27	39.06	32.31	65.23	24.63	77.75	94.28	81.91	99.14	97.68	98.11	57.43	78.66	49.08	-	-	-
SparseMVC	87.95	94.81	86.75	35.65	59.15	32.98	52.55	66.91	38.98	24.87	62.74	23.79	89.15	96.88	89.42	97.86	94.23	95.31	42.14	73.74	37.00	14.44	63.73	7.46
HSACC	84.86	92.24	82.37	33.39	56.47	27.86	51.81	63.11	37.93	25.05	53.91	16.60	96.30	98.71	96.25	92.55	93.99	88.77	64.36	81.44	56.61	-	-	-
MCMC	51.43	87.18	62.15	35.48	62.72	33.73	29.15	58.17	25.73	14.16	61.46	17.07	36.02	77.22	35.70	99.25	97.92	98.35	13.96	67.14	19.63	7.50	49.81	4.07
TURTLE	92.59	93.80	87.62	45.01	65.02	36.89	57.55	68.42	42.69	36.78	60.80	25.76	99.56	99.68	99.48	99.50	98.56	98.90	89.10	91.35	82.46	70.10	86.58	58.42
MSRL	95.83	95.83	92.14	49.78	65.89	46.65	62.34	72.89	49.03	37.65	66.96	27.72	99.71	99.76	99.58	99.57	98.74	99.05	91.00	92.34	84.72	73.24	88.26	62.80

TABLE III: Clustering performance of MSRL using different combinations of pretrained models across eight vision datasets.

Model	Models	Pets			GTSRB			DTD			Aircraft			Flowers			CIFAR-10			CIFAR-100			ImageNet		
		L/14B	16B	32	ACC	NMI	ARI	ACC	NMI	ARI	ACC	NMI	ARI	ACC	NMI	ARI	ACC	NMI	ARI	ACC	NMI	ARI	ACC	NMI	ARI
DINOv2	✓	95.83	95.83	92.14	49.78	65.89	46.65	62.34	72.89	49.03	37.65	66.96	27.72	99.71	99.76	99.58	99.57	98.74	99.05	91.00	92.34	84.72	73.24	88.26	62.80
	✓	93.35	94.41	89.48	41.65	58.80	36.01	62.66	72.44	49.08	33.54	64.42	24.53	99.74	99.79	99.64	99.41	98.27	98.69	88.43	90.78	80.98	71.46	87.30	60.25
	✓	93.30	94.19	88.36	41.16	58.92	33.93	60.74	70.79	46.60	35.61	65.92	26.75	99.76	99.80	99.66	99.37	98.18	98.61	86.79	89.95	79.05	71.05	87.15	59.78
	✓	96.46	96.47	93.60	47.02	66.52	42.01	64.95	75.21	52.57	40.35	70.03	31.57	99.79	99.82	99.72	99.47	98.45	98.83	89.60	91.44	82.88	72.97	88.11	62.30
	✓	94.96	95.53	91.12	45.96	64.57	41.31	64.36	74.64	52.10	40.47	69.21	31.72	99.76	99.80	99.68	99.46	98.40	98.81	89.23	91.35	82.47	72.40	87.69	61.31
	✓	95.50	95.45	91.54	47.92	69.02	41.41	66.22	75.68	53.97	39.24	68.26	30.58	99.76	99.81	99.69	99.40	98.25	98.67	88.71	90.86	81.24	70.46	87.12	59.73

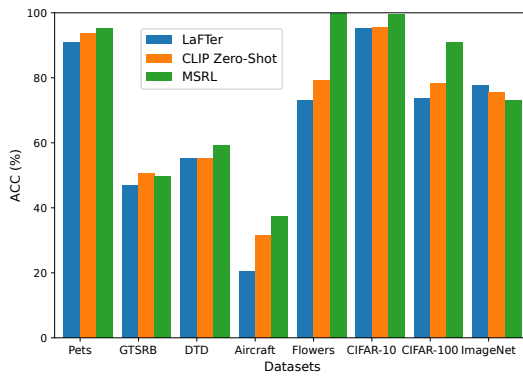


Fig. 2: Clustering accuracy comparison between MSRL and the zero-shot transfer learning-based methods.

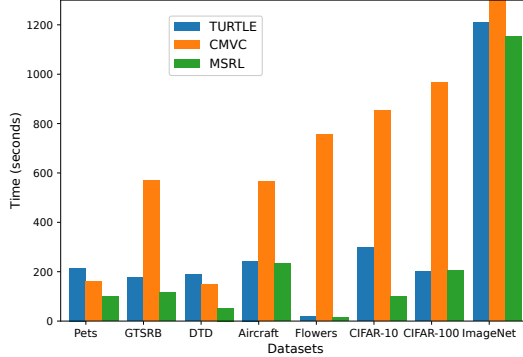


Fig. 3: Training time comparison (in seconds) among MSRL, TURTLE and CMVC for eight vision datasets.

1) Self-Supervised Learning: The experimental results of all the competing methods on the self-supervised learning task are listed in Table II. The symbol ‘-’ in Table II indicates that the competing method encounters from out of memory errors when clustering is performed on a given vision dataset. The best and second-best clustering results are highlighted in bold and underlined, respectively. MSRL consistently outperforms the competing methods across all eight vision datasets. For example, it achieves ACC values of 91.00% and 73.24%

on the CIFAR-100 and ImageNet datasets, respectively. It significantly outperforms the other competing methods by at least 1.9% and 3.14% in terms of the ACC. Moreover, MSRL also exhibits consistent advantages across the other three evaluation metrics. In addition, TURTLE achieves competitive clustering results over the multiview clustering approaches across all vision datasets. In contrast, the multiview clustering approaches generally yield less competitive clustering results, especially for large-scale vision datasets such as CIFAR-100 and ImageNet. These clustering results demonstrate the effectiveness of the proposed MSRL approach for self-supervised learning tasks.

The advantages of the proposed MSRL approach can be attributed to two key factors. First, high-level semantic knowledge is effectively transferred by leveraging multiple pretrained models, which also reduces excessive memory consumption. Second, complementary information across multiple views is explicitly exploited by enforcing consistency among assignment probability distributions, thereby mitigating the adverse effects of distribution heterogeneity across views. In contrast, traditional multiview clustering approaches typically assume homogeneous feature spaces or depend on direct feature fusion strategies, which limits their effectiveness when handling heterogeneous representations.

2) Zero-Shot Transfer Learning: We compare MSRL with zero-shot transfer learning methods that utilize descriptions of ground truth classes as a form of supervision, including CLIP zero-shot transfer [10] and LaFTer [13]. The clustering accuracy comparison between MSRL and the zero-shot transfer learning-based methods is shown Fig. 2. MSRL outperforms CLIP zero-shot transfer and LaFTer on all eight vision datasets except GTSRB and ImageNet. The descriptions of the ground-truth classes provide effective external supervision for zero-shot transfer learning, which narrows the performance gap for the GTSRB and ImageNet datasets. This finding can be attributed to the strong semantic alignment between class-level textual descriptions and the pretraining distribution of CLIP-based models on these datasets. In contrast,

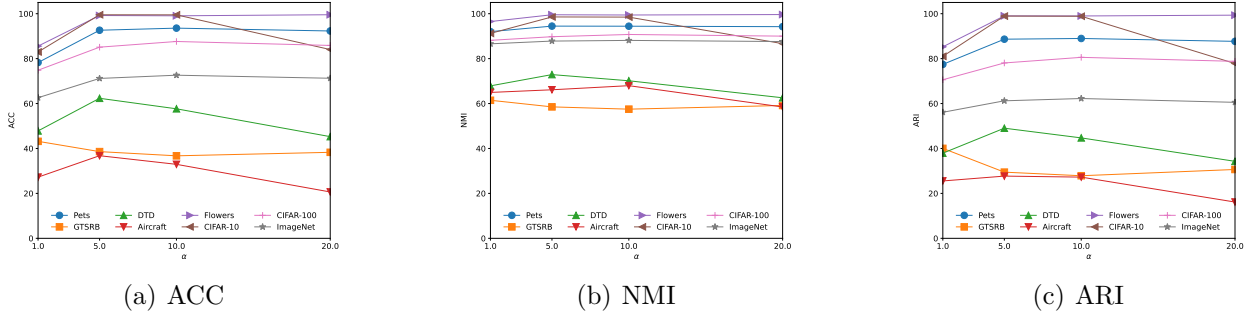
Fig. 4: Clustering results on eight vision datasets with different values of  $\alpha$  in Eq. (14).

TABLE IV: Ablation study of the main components in Eq. (14) with eight vision datasets.

Methods	$\mathcal{L}_s$	$\mathcal{L}_a$	$\mathcal{L}_c$	Pets			GTSRB			DTD			Aircraft			Flowers			CIFAR-10			CIFAR-100			ImageNet		
				ACC	NMI	ARI	ACC	NMI	ARI	ACC	NMI	ARI	ACC	NMI	ARI	ACC	NMI	ARI	ACC	NMI	ARI	ACC	NMI	ARI	ACC	NMI	ARI
MSRL <sub>avg</sub>	✓	✓		90.05	92.73	85.27	40.00	56.25	29.79	54.47	68.31	42.30	29.25	57.66	20.89	99.20	99.64	99.42	99.37	98.17	98.61	84.82	88.82	77.22	72.31	88.27	62.47
MSRL	✓	✓	✓	95.26	95.15	91.10	49.60	65.73	46.51	59.20	69.23	44.95	37.44	65.46	28.18	99.71	99.76	99.58	99.57	98.74	99.05	90.95	92.30	84.61	73.21	88.25	62.77

MSRL does not depend on class-level semantic descriptions. Instead, it learns invariant representations from large-scale unlabeled visual data with various pretrained models in a fully unsupervised transfer manner. These invariant representations enable more flexible adaptation to diverse visual domains. Consequently, MSRL demonstrates strong robustness even in scenarios where explicit semantic supervision is available.

### C. Training Time Comparison on Self-Supervised Learning

To validate the optimization efficiency of the proposed MSRL approach, we compare the training times among MSRL, TURTLE and SparseMVC on all eight vision datasets. These training times are presented in Fig. 3. It can be observed that both MSRL and TURTLE significantly outperform SparseMVC in terms of training time, where SparseMVC is considered a representative method for multiview clustering. This efficiency gain can be attributed to the use of unsupervised transfer learning, which helps reduce the computational cost associated with handling raw image data. By leveraging pretrained models, both MSRL and TURTLE benefit from reduced complexity when handling high-dimensional visual features, leading to faster convergence during training. Moreover, MSRL consistently runs faster than TURTLE on most of the datasets, which can be attributed to its ability to achieve competitive performance with fewer iterations.

### D. Parameter Sensitivity Analysis

The semantic pseudolabel loss  $\mathcal{L}_s$  and the cross-view consistency loss  $\mathcal{L}_c$  in Eq. (14) are closely related to the assignment probability distributions of the samples. The parameter  $\beta$  was empirically fixed at 1.0, while the hyperparameter  $\alpha$  was selected from  $\{1.0, 5.0, 10.0, 20.0\}$ . The remaining hyperparameters in the proposed MSRL method were determined according to the experimental settings. The clustering performance, including the ACC,

NMI, and ARI, on the eight vision datasets under different values of  $\alpha$  is shown in Fig. 4. The experimental results indicate that the proposed MSRL method achieves stable and strong performance when  $\alpha$  is chosen from  $\{1.0, 5.0, 10.0\}$ .

### E. Ablation Study

The semantic pseudolabel loss  $\mathcal{L}_s$  and the cluster diversity loss  $\mathcal{L}_a$  are two essential components of the overall loss in Eq. (14). In addition, the cross-view consistency loss  $\mathcal{L}_c$  is incorporated to enforce consistency among assignment probability distributions across heterogeneous views, which facilitates the learning of invariant representations. To investigate the impact of the cross-view consistency loss  $\mathcal{L}_c$  in Eq. (14), we conduct an ablation study for the eight vision datasets. Specifically, we construct a variant of the proposed model that omits  $\mathcal{L}_c$  and employs only  $\mathcal{L}_s$  and  $\mathcal{L}_a$  in the overall loss, denoted as MSRL<sub>avg</sub>. Table IV shows the clustering performance comparison between MSRL and MSRL<sub>avg</sub>. The ablation results show that MSRL consistently outperforms MSRL<sub>avg</sub> across all the evaluated datasets. This finding demonstrates the effectiveness of the cross-view consistency loss. These results indicate that  $\mathcal{L}_c$  enhances assignment probability distribution consistency across multiple views, which in turn leads to significant performance improvements for the proposed MSRL method.

### F. Evaluation of the Increasing Number of Pretrained Models

The clustering performance of MSRL is influenced by the number of incorporated pretrained models, since different pretrained models correspond to heterogeneous views. To investigate the effect of varying the number of views, we conduct an additional ablation study with progressively constructed model combinations. Specifically, DINOv2 ViT-g/14 is fixed as a core pretrained model, and alternative pretrained models are incrementally selected from ViT-B/32, ViT-B/16 and ViT-L/14, which results

in five different combinations with increasing numbers of views. This experimental protocol enables a controlled evaluation of how clustering performance evolves as more views are incorporated. All the hyperparameters of MSRL are kept identical to those specified in the experimental settings.

Table III presents the clustering performance of MSRL under different combinations of pretrained models across eight vision datasets, which provides empirical validation for the incremental view analysis. When DINOv2 ViT-g/14 is combined with a single alternative pretrained model, ViT-L/14 almost emerges as the optimal choice. Moreover, the combination of DINOv2 ViT-g/14 and ViT-B/16 almost outperforms that of DINOv2 ViT-g/14 and ViT-B/32. This finding indicates that the quality of the additional view plays a critical role. When the number of pretrained models increases to three, the combination including ViT-L/14 and ViT-B/16 yields better clustering performance than the alternative combination including ViT-L/14 and ViT-B/32 does. However, when all four pretrained models are incorporated, the clustering performance is not the most competitive. Overall, these findings demonstrate that not every additional view is guaranteed to be beneficial for MSRL. In particular, lower-quality pretrained models such as ViT-B/32 may negatively affect clustering performance. Consequently, the clustering performance of MSRL can decrease as the number of views increases if low-quality pretrained models are included, which highlights the importance of both view quality and the integration of model selection.

## V. Conclusion

In this paper, we present the MSRL method for multiview self-representation learning across heterogeneous views. We introduce an information-passing mechanism that leverages self-representation learning to perform a feature aggregation operation on linear features, enabling information aggregation from spatially proximate neighbors. In addition, an assignment probability distribution consistency scheme is incorporated to enforce consistency among assignment probability distributions across multiple views. This approach enables complementary information to be effectively captured in multiview self-representation learning. The proposed MSRL method learns invariant representations across different linear models. Furthermore, we provide a theoretical analysis of the information-passing mechanism, the assignment probability distribution consistency and the incremental views. Extensive experiments on multiple benchmark visual datasets demonstrate that the proposed MSRL method consistently outperforms several state-of-the-art approaches.

## References

- [1] W. Hu, Y. Yang, and H. Hu, “Pseudo label association and prototype-based invariant learning for semi-supervised NIR-VIS face recognition,” *IEEE Trans. Image Process.*, vol. 33, pp. 1448–1463, 2024.
- [2] D. Hegde, S. Lohit, K. Peng, M. Jones, and V. Patel, “Multi-modal 3d object detection on unseen domains,” in in Proc. IEEE Conf. Comput. Vis. Pattern Recognit., Jun. 2025, pp. 524–2534.
- [3] J. Pang, N. Tang, K. Li, Y. Tang, X. Cai, Z. Zhang, G. Niu, M. Sugiyama, and Y. Yu, “Learning view-invariant world models for visual robotic manipulation,” in in Proc. 13th Int. Conf. Learn. Represent., Jul. 2025, pp. 1–24.
- [4] J. Gui, T. Chen, J. Zhang, Q. Cao, Z. Sun, and H. Luo, “A survey on self-supervised learning: Algorithms, applications, and future trends,” *IEEE Trans. Pattern Anal. and Mach. Intell.*, vol. 46, no. 12, pp. 9052–9071, Dec. 2024.
- [5] K. You, Y. Liu, J. Wang, and M. Long, “Logme: Practical assessment of pre-trained models for transfer learning,” in in Proc. 38th Int. Conf. Mach. Learn., Jul. 2021, pp. 12133–12143.
- [6] Z. Liu, Y. Xu, Y. Xu, Q. Qian, H. Li, X. Ji, A. B. Chan, and R. Jin, “Improved fine-tuning by better leveraging pre-training data,” in in Proc. 36th Adv. Neural Inf. Process. Syst., New Orleans, Louisiana, USA, Dec. 2022, pp. 32568–32581.
- [7] A. Abduweili, X. Li, H. Shi, C. Xu, and D. Dou, “Adaptive consistency regularization for semi-supervised transfer learning,” in in Proc. IEEE Conf. Comput. Vis. Pattern Recognit., Jun. 2021, pp. 6923–6932.
- [8] T. Darcet, M. Oquab, J. Mairal, and P. Bojanowski, “Vision transformers need registers,” in in Proc. 12th Int. Conf. Learn. Represent., Jul. 2024, pp. 1–21.
- [9] J. Z. HaoChen, C. Wei, A. Kumar, and T. Ma, “Beyond separability: analyzing the linear transferability of contrastive representations to related subpopulations,” in in Proc. 36th Adv. Neural Inf. Process. Syst., New Orleans, Louisiana, USA, Dec. 2022, pp. 26889–26902.
- [10] A. Gadetsky, Y. Jiang, and M. Brbic, “Let go of your labels with unsupervised transfer,” in in Proc. 41th Int. Conf. Mach. Learn., Vienna, Austria, Jul. 2024, pp. 14382–14407.
- [11] B. Alkin, L. Miklautz, S. Hochreiter, and J. Brandstetter, “Mim-refiner: A contrastive learning boost from intermediate pre-trained representations,” in in Proc. 13th Int. Conf. Learn. Represent., Jul. 2025, pp. 1–37.
- [12] H. Chen, Z. Huang, Y. Hong, Y. Wang, Z. Lyu, Z. Xu, J. Lan, and Z. Gu, “Efficient transfer learning for video-language foundation models,” in in Proc. IEEE Conf. Comput. Vis. Pattern Recognit., Jun. 2025, pp. 29129–29138.
- [13] M. J. Mirza, L. Karlinsky, W. Lin, H. Possegger, M. K. R. Feris, and H. Bischof, “LaFTer: Label-free tuning of zero-shot classifier using language and unlabeled image collections,” in in Proc. 37th Adv. Neural Inf. Process. Syst., New Orleans, Louisiana, USA, Dec. 2023, pp. 5763–5777.
- [14] C. Du, Y. Wang, S. Song, and G. Huang, “Probabilistic contrastive learning for long-tailed visual recognition,” *IEEE Trans. Pattern Anal. and Mach. Intell.*, vol. 46, no. 9, pp. 5890–5904, Sept. 2024.
- [15] Y. Tian, L. Fan, K. Chen, D. Katabi, D. Krishnan, and P. Isola, “Learning vision from models rivals learning vision from data,” in in Proc. IEEE Conf. Comput. Vis. Pattern Recognit., Jun. 2024, pp. 15887–15898.
- [16] A. Oord, Y. Li, and O. Vinyals, “Representation learning with contrastive predictive coding,” in arXiv preprint arXiv:1807.03748, Jan. 2019, pp. 1–13.
- [17] R. D. Hjelm, A. Fedorov, S. Lavoie-Marchildon, K. Grewal, P. Bachman, A. Trischler, and Y. Bengio, “Learning deep representations by mutual information estimation and maximization,” in in Proc. 9th Int. Conf. Learn. Represent., Jul. 2021, pp. 1–24.
- [18] W. Huang, A. Han, Y. Chen, Y. Cao, Z. Xu, and T. Suzuki, “On the comparison between multi-modal and single-modal contrastive learning,” in in Proc. 37th Adv. Neural Inf. Process. Syst., Vancouver, BC, Canada, Dec. 2024, pp. 81549–81605.
- [19] T. Wang and P. Isola, “Understanding contrastive representation learning through alignment and uniformity on the hypersphere,” in in Proc. 39th Int. Conf. Mach. Learn., Jul. 2020, pp. 9929–9939.
- [20] Y. Tian, C. Sun, B. Poole, D. Krishnan, C. Schmid, and P. Isola, “What makes for good views for contrastive learning,” in in Proc. 34th Adv. Neural Inf. Process. Syst., Vancouver, Canada, Dec. 2020, pp. 6827–6839.
- [21] T. Chen, S. Kornblith, M. Norouzi, and G. Hinton, “A simple framework for contrastive learning of visual representations,” in in Proc. 37th Int. Conf. Mach. Learn., Jul. 2020, pp. 1597–1607.

[22] Y. Xin, J. Du, Q. Wang, Z. Lin, and K. Yan, "VMT-Adapter: Parameter-efficient transfer learning for multi-task dense scene understanding," in in Proc. AAAI Conf. Artif. Intell., Vancouver, British Columbia, Canada, Feb. 2024, pp. 16 085–16 093.

[23] J. Chen, H. Mao, Y. Gou, and X. Peng, "Hierarchical sparse representation clustering for high-dimensional data streams," IEEE Trans. Neural. Netw. Learn. Syst., vol. 36, no. 10, pp. 18 035–18 047, Oct. 2025.

[24] J. Chen, S. Yang, H. Mao, and C. Fahy, "Multiview subspace clustering using low-rank representation," IEEE Trans. Cybern., vol. 52, no. 11, pp. 12 364–12 378, Nov. 2022.

[25] J. Chen, S. Yang, Z. Wang, and H. Mao, "Efficient sparse representation for learning with high-dimensional data," IEEE Trans. Neural. Netw. Learn. Syst., vol. 34, no. 8, pp. 4208–4222, Aug. 2023.

[26] L. Fu, Z. Chen, Y. Chen, and S. Wang, "Unified low-rank tensor learning and spectral embedding for multi-view subspace clustering," IEEE Trans. Multi., vol. 25, pp. 4972–4985, Jun. 2022.

[27] R. Liu, X. Zou, C. Tang, X. Zheng, X. Hu, K. Sun, and X. Liu, "SparseMVC: probing cross-view sparsity variations for multi-view clustering," in in Proc. 39th Adv. Neural Inf. Process. Syst., San Diego, USA, Dec. 2025, pp. 1–29.

[28] J. Chen, H. Mao, W. L. Woo, and X. Peng, "Deep multiview clustering by contrasting cluster assignments," in in Proc. IEEE/CVF Int. Conf. Comput. Vis., Paris, France, Oct. 2023, pp. 16 752–16 761.

[29] L. Fu, B. Deng, S. Huang, T. Liao, C. Zhang, and C. Chen, "Learn from global rather than local: consistent context-aware representation learning for multi-view graph clustering," in in Proc. 34th Int. Joint Conf. Artif. Intell., Montreal, Canada, Aug. 2025, pp. 5145–5153.

[30] B. Deng, T. Wang, L. Fu, S. Huang, C. Chen, and T. Zhang, "THESAURUS: contrastive graph clustering by swapping fused gromov-wasserstein couplings," in in Proc. AAAI Conf. Artif. Intell., Philadelphia, Pennsylvania, USA, Feb. 2025, pp. 16 199–16 207.

[31] P. Veličković, G. Cucurull, A. Casanova, A. Romero, P. Li.o, and Y. Bengio, "Graph attention networks," in Proc. 6th Int. Conf. Learn. Represent., Vancouver, BC, Canada, Apr. 2018, pp. 1–12.

[32] J. Wen, S. Deng, W. Wong, G. Chao, C. Huang, L. Fei, and Y. Xu, "Diffusion-based missing-view generation with the application on incomplete multi-view clustering," in in Proc. 41th Int. Conf. Mach. Learn., Vienna, Austria, Jul. 2024, pp. 52 762–527.

[33] C. Luo, J. Xu, Y. Ren, J. Ma, and X. Zhu, "Simple contrastive multi-view clustering with data-level fusion," in in Proc. 33th Int. Joint Conf. Artif. Intell., Jeju Island, South Korea, Aug. 2024, pp. 4697–4705.

[34] M. Belkin and P. Niyogi, "Laplacian eigenmaps for dimensionality reduction and data representation," Neural Comput., vol. 15, no. 6, pp. 1373–1396, Jun. 2003.

[35] A. Vaswani, N. Shazeer, N. Parmar, J. Uszkoreit, L. Jones, A. N. Gomez, L. Kaiser, and I. Polosukhin, "Attention is all you need," in in Proc. 31th Adv. Neural Inf. Process. Syst., Long Beach, California, USA, Dec. 2017, pp. 1–11.

[36] J. Xu, H. Tang, Y. Ren, L. Peng, X. Zhu, and L. He, "Multi-level feature learning for contrastive multi-view clustering," in in Proc. IEEE Conf. Comput. Vis. Pattern Recognit., New Orleans, Louisiana, USA, Jun. 2022, pp. 16 051–16 060.

[37] D. P. Kingma and J. L. Ba, "ADAM: a method for stochastic optimization," in Proc. 3th Int. Conf. Learn. Represent., San Diego, CA, USA, May 2015, pp. 1–15.

[38] H. Robbins and S. Monro, "A stochastic approximation method," Ann. Math. Statist., vol. 22, no. 3, pp. 400–407, Sept. 1954.

[39] M. Oquab, T. Darcet, T. Moutakanni, and et.al, "DINOv2: Learning robust visual features without supervision," in In Trans. Mach. Learn. Res., Jan. 2024, pp. 1–32.

[40] A. Radford, J. W. Kim, C. Hallacy, A. Ramesh, G. Goh, S. Agarwal, , and et.al, "Learning transferable visual models from natural language supervision," in in Proc. 38th Int. Conf. Mach. Learn., Online, Jul. 2021, pp. 8748–8763.

[41] A. Paszke, S. Gross, F. Massa, A. Lerer, J. Bradbury, G. Chanan, and et.al, "Pytorch: an imperative style, high-performance deep learning library," in in Proc. 33th Adv. Neural Inf. Process. Syst., Vancouver, BC, Canada, Dec. 2019, pp. 1–12.

[42] Y. Zhang, W. Yan, C. Tang, W. Zhou, and J. Jin, "Multi-branch space sharing feature aggregation for contrastive multi-view clustering," Pattern Recognit., vol. 167, p. 111704, Nov. 2025.

[43] R. Liu, X. Zou, C. Tang, X. Zheng, X. Hu, K. Sun, and X. Liu, "SparseMVC: Probing cross-view sparsity variations for multi-view clustering," in in Proc. 39th Adv. Neural Inf. Process. Syst., San Diego, USA, Dec. 2025, pp. 1–29.

[44] X. Ding, L. Zhao, X. Li, and X. Zhu, "Incomplete multi-view clustering via hierarchical semantic alignment and cooperative completion," in in Proc. 39th Adv. Neural Inf. Process. Syst., San Diego, USA, Dec. 2025, pp. 1–21.

[45] J. Bian, Y. Lin, X. Xie, C. Wang, L. Yang, J. Lai, and F. Nie, "Multilevel contrastive multiview clustering with dual self-supervised learning," IEEE Trans. Neural. Netw. Learn. Syst., vol. 36, no. 6, pp. 10 422–10 436, Jun. 2025.